Rapid prediction of fuel research octane number and octane sensitivity using the AFIDA constant-volume combustion chamber

Jon Luecke, Bradley T. Zigler

National Renewable Energy Laboratory, 15013 Denver West Parkway, Golden, CO 80401, USA

***Corresponding author. Email address: jon.luecke@nrel.gov**

Abstract

Current research octane number (RON) and motor octane number (MON) gasoline performance characterization techniques use dated, complex engine testing methodology and limit researchers' ability to easily characterize small volumes of experimental fuels. A novel methodology is presented that correlates measured ignition delay (ID) time to RON in an Advanced Fuel Ignition Delay Analyzer (AFIDA) constant-volume combustion chamber device at a single pressure/temperature condition, with an r^2 of 0.99 and standard error (SE) of 1.0. The correlation of the slope of the ID time between two additional temperature points to octane sensitivity (S) produces an r^2 of 0.97 and SE of 0.69; however, fuels with S > 12 are indistinguishable. These results are based on methodology calibration using 31 primary and toluene reference fuels containing 0%–40% ethanol with RON values ranging from 85–113. Validation of these methods using a 102-sample fuel matrix spanning an array of base fuels and additive chemistry designed to test the robust applicability of the method, along with pump gasoline and high-octane surrogate blend samples, demonstrates an r^2 of 0.94 and SE of 1.3 for the RON correlation over all samples, whereas the equivalent S correlation produces an r^2 of 0.78 and SE of 1.2 by excluding two additives, 3-pentanone and diisobutylene, which displayed poor S correlation results. This novel AFIDA analysis method can be performed in 1 hour and with 40 mL of fuel, offering significant improvements in time and volume requirements over traditional techniques.

Keywords: AFIDA, constant-volume combustion chamber, fuel, octane number, gasoline, combustion

Abbreviations

AFIDA – Advanced Fuel Ignition Delay Analyzer

CFR – Cooperative Fuel Research

CN – cetane number

CVCC – constant-volume combustion chamber

DCN – derived cetane number

E30 – 30% ethanol blend by volume

HPLC – high-pressure liquid chromatography

ID – ignition delay

K – weighting factor constant depending on pressure/temperature histories with time in an end gas

MON – motor octane number

NTC – negative temperature coefficient

OI – octane index (OI = RON – K×S)

PRF – primary reference fuel

RON – research octane number

S – octane sensitivity (RON – MON)

SE – standard error

TRF – toluene reference fuel

ϕ – fuel-air equivalence ratio (phi)

1. Introduction

Spark-ignition engine fuel is rated based on its ability to withstand in-cylinder heat and pressure without autoigniting a portion of the fuel-air mixture ahead of the flame front, an undesirable event known as "knocking" or "pinging" due to its audible signature [1]. This phenomenon produces high-pressure

shockwaves that can damage engine components if unmitigated, therefore limiting maximum operational compression ratio, ignition timing, and engine thermal efficiency. Current gasoline fuel antiknock quality characterization techniques dates back to research octane number (RON) and motor octane number (MON) Cooperative Fuel Research (CFR) engine-based tests developed in the 1920s, whereby an operator adjusts compression ratio under defined conditions on the single-cylinder carbureted engine and measures maximum knock, which is then compared to similar results obtained from a mixture of iso-octane and n-heptane, two primary reference fuels (PRFs) that define the octane scale [2–4]. Together, the RON test—which simulates low-speed, high-load conditions (600 RPM, ambient intake temperature, etc.)—and the MON test—which simulates high-speed, high-load conditions (900 RPM, heated intake temperature, etc.)—describe a fuel's ability to withstand autoignition over two different pressure-temperature trajectories. They pose many drawbacks for fuel researchers, however, including the requirement of 0.5 liters of fuel per test, time and cost to send samples to a limited number of laboratories with the specialized hardware and training to perform the test, failure to incorporate modern technology into the test apparatus, and the limitation of using two pressure-temperature trajectories to completely describe a fuel's antiknock quality, which may not effectively correlate to fuel performance for a variety of modern engine operating conditions [5].

For some time, RON and MON metrics alone are known to be flawed in sufficiently describing antiknock fuel performance in modern engines. Octane index (OI = RON – K×S), which incorporates an additional engine operating condition parameter K, along with octane sensitivity (S), the difference between RON and MON (S = RON – MON), relates relative contributions of RON and MON based on engine operating conditions to antiknock quality with better results [6]. Over time, engines have been shown to be increasingly operating with negative K values due to improved breathing, cooling, downsizing, and downspeeding technologies, making high-RON and low-MON (high-S) fuels desirable [7]. Fuel-air mixtures in modern spark-ignition direct injection gasoline engines undergo different thermodynamic

pressure-temperature trajectories than those bounded by RON and MON, resulting in high fuel knock resistance being more accurately described for boosted direct injection engines by OI with a negative K value that favors high S [8]. A large portion of S magnitude is determined by a fuel's negative temperature coefficient (NTC) kinetic region, whereby the reaction rate is inversely proportional to temperature over the range of approximately 700–900 K, depending on pressure and fuel chemistry. Fuels such as paraffinic hydrocarbons, which exhibit NTC behavior, tend to present little to no S and exhibit two-stage autoignition, whereas fuels such as ethanol, which do not exhibit NTC chemistry, present very high S and single-stage autoignition [9]. Fuels with high S have chemical kinetics that inhibit the portion of ignition kinetics known as cool flame activity [10]. NTC chemistry or lack thereof is therefore a good predictor of fuel sensitivity, which in turn is a good indicator for fuel antiknock quality in modern engines [9].

The last 15 years have seen significant methodology changes in analyzing compression-ignition (diesel) fuel combustion quality by way of measuring a derived cetane number (DCN). Until then, CFR engine-based methodology was unchallenged, but recent adaptations of multiple constant-volume combustion chamber (CVCC) devices to correlate ignition delay (ID) results to cetane number (CN) have been very successful, leading to multiple ASTM-approved standards [11–14]. Other researchers have recently developed methods to correlate CVCC-based ignition delay times for gasoline-range fuel blends over temperature sweeps to RON, MON, and OI [15,16].

The National Renewable Energy Laboratory recently characterized and developed the commercially available Advanced Fuel Ignition Delay Analyzer (AFIDA) CVCC for the validation of gasoline-range fuel chemical kinetic modeling, which demonstrated the ability of the device to capture NTC chemistry kinetics of gasoline-range fuels over a specific range of engine-relevant pressure and temperature conditions [17]. The incorporation of a modern piezoelectric diesel injector and compatibility of

gasoline-range fuels with the AFIDA makes it possible to attempt gasoline-range fuel knock resistance correlative pursuits. Building upon previous work, well-characterized experiments were carried out in the device to empirically determine if ID time measurements from specific pressure-temperature conditions exist that could be used to correlate to RON, MON, and S.

This paper presents ID time data measured at specific temperature and pressure conditions from the AFIDA device, correlated to measured RON and S values for a wide variety of fuel chemistry combinations. This comprehensive empirical evaluation illustrates how this technique can be used to evaluate gasoline fuel quality for researchers working with fuel compounds and blends for which only very limited fuel quantity (~40 mL) may be available from novel synthesis or catalytic processes, or as a faster screening alternative for gasoline fuel antiknock quality. Along with providing a correlation to the traditional gasoline-range fuel antiknock quality characterization approach, this technique lays the foundation for future combustion characterization metrics based on CVCC ID times that may be more relevant or tailored to specific modern engine operating conditions and easier to perform than the traditional CFR engine-based methodologies.

2. Materials and methods

2.1 Materials

The research-grade AFIDA device was purchased from ASG Analytik-Service Gesellschaft mbH. MilliporeSigma supplied the iso-octane (2,2,4-trimethylpentane 99.8% CAT# 360066), n-heptane (99% HPLC Plus CAT# 650536), toluene (99.8% anhydrous CAT# 244511), and ethanol (pure 200 proof CAT# 459844) used for making PRF and toluene reference fuel (TRF) blends. Infineum International Limited supplied the R655 lubricity additive sample. Matheson Tri-Gas, Inc. supplied the primary standard 20.9% (molar volume) oxygen balance nitrogen air cylinders used for charge air.

2.2 Fuel blending procedure

A gravimetric approach was used to blend fuels directly into sample vials, which was expected to improve final blend accuracy compared to a volumetric approach, which involves increased fuel handling and associated evaporation for volatile components. For each blend, target weights were determined based on the density for each component and target fuel composition. Individual fuel components were then weighed directly into 40-mL AFIDA-compatible sample vials, taring the scale before each new component was added. A Mettler Toledo PB303-S analytical balance was used to weigh target fuel amounts, which were weighed to within 5 mg for each component target.

2.3 AFIDA experimental overview

ID measurement experiments were performed using a research-grade AFIDA CVCC, where a precise amount of fuel is injected at 1,190-bar initial pressure through a top centrally mounted modern 7-hole CRI3-18-based Bosch piezoelectric fuel injector into a well-controlled heated and pressurized symmetrical 0.4-L chamber, resulting in autoignition. A high-pressure liquid chromatography (HPLC)-type dual-piston fuel pump supplies precise initial pressure to a small, fixed-volume fuel system, but unlike a typical common rail direct fuel injection system found in vehicles, fuel pressure drops during the injection event because the HPLC pump is unable to supply pressure during the user-defined injection duration up to 5 ms. For example, a 4 ms injection duration which begins with 1190 bar initial fuel line pressure ends with a final fuel line and injection pressure of ~300 bar, as fuel pressure drops continuously as the injection event proceeds. This setup offers the advantage of small fuel volume requirements but limits the maximum amount of fuel that can be injected. All fuel samples were doped with 1,000–2,000 parts per million by volume Infineum R655, a lubricity additive used to improve the piezoelectric diesel injector's operability when using gasoline-range fuels [17,18]. Comprehensive AFIDA device and experimental details, which include uncertainty analysis [17], have been previously well documented [19]. ID time, defined as the time lapse between start of injection and start of ignition, is derived from chamber pressure data recorded using a liquid cooled Kistler 6041B pressure transducer.

The electronic triggering signal determines a fixed start of injection time, which is verified against pressure data. Start of ignition is defined as the time at which the chamber pressure reaches 40% of the maximum pressure for each individual injection event. Fig. 1 shows a simplified schematic of the AFIDA device and Fig. 2 shows an example of pressure data obtained from a single injection event. The test temperature, used to define the experimental temperature condition, is measured using the average of two equidistant off-center class 2, type K (nickel-chromium/nickel-alumel) thermocouples mounted through the bottom of the combustion chamber, as illustrated in Fig 1. It has been observed that the actual average internal air temperature within the AFIDA is approximately 25°C lower than the test temperature [17]. ID data points are plotted using the average of 12 individual injection events unless outliers are determined, in which case they are removed from the calculated average, the same approach used in ASTM D8183, Standard Test Method for Determination of Indicated Cetane Number (ICN) of Diesel Fuel Oils using a Constant Volume Combustion Chamber, where the measured ID time from the AFIDA device is correlated to cetane number [14].

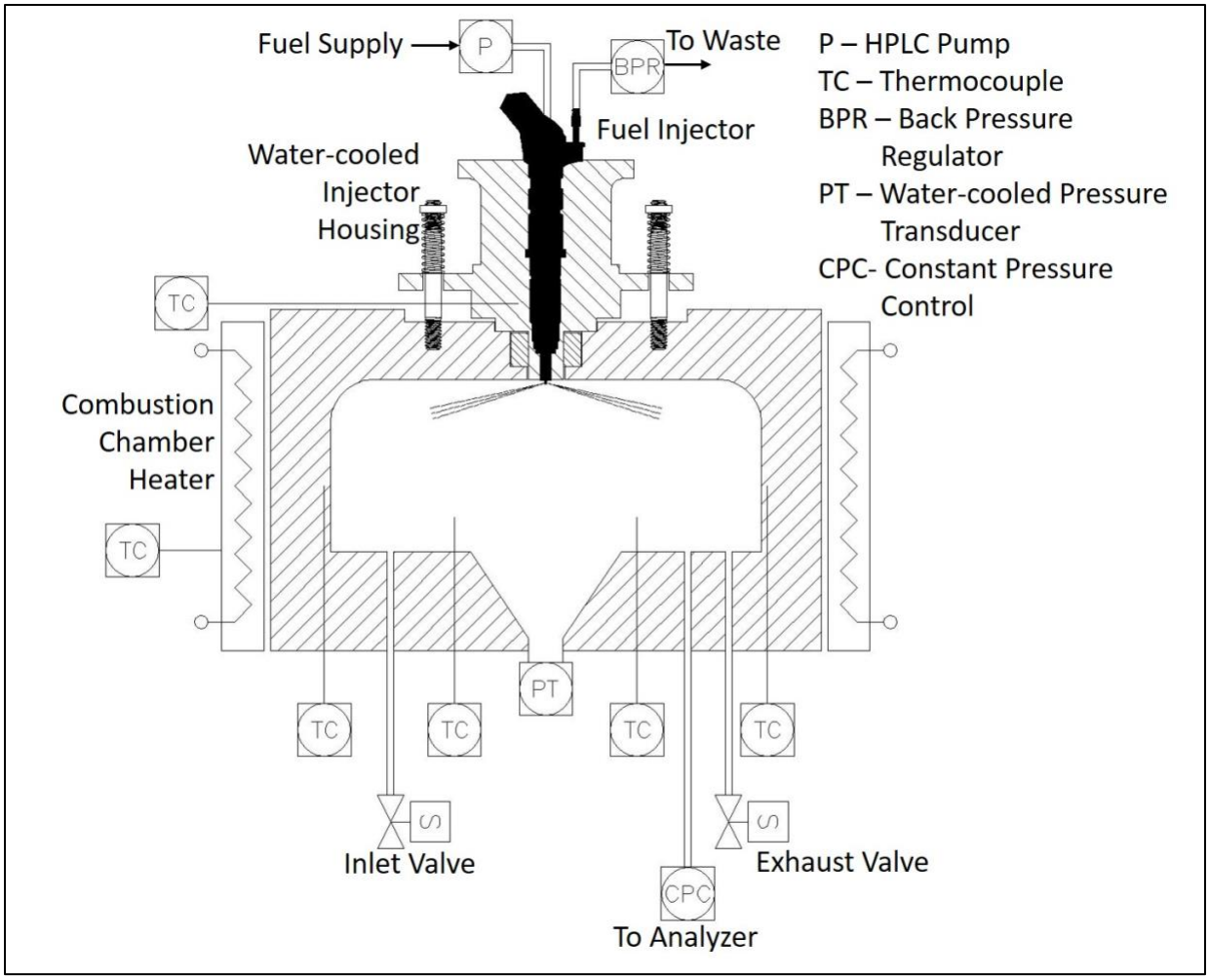

157

158 Fig. 1. Simplified AFIDA schematic.

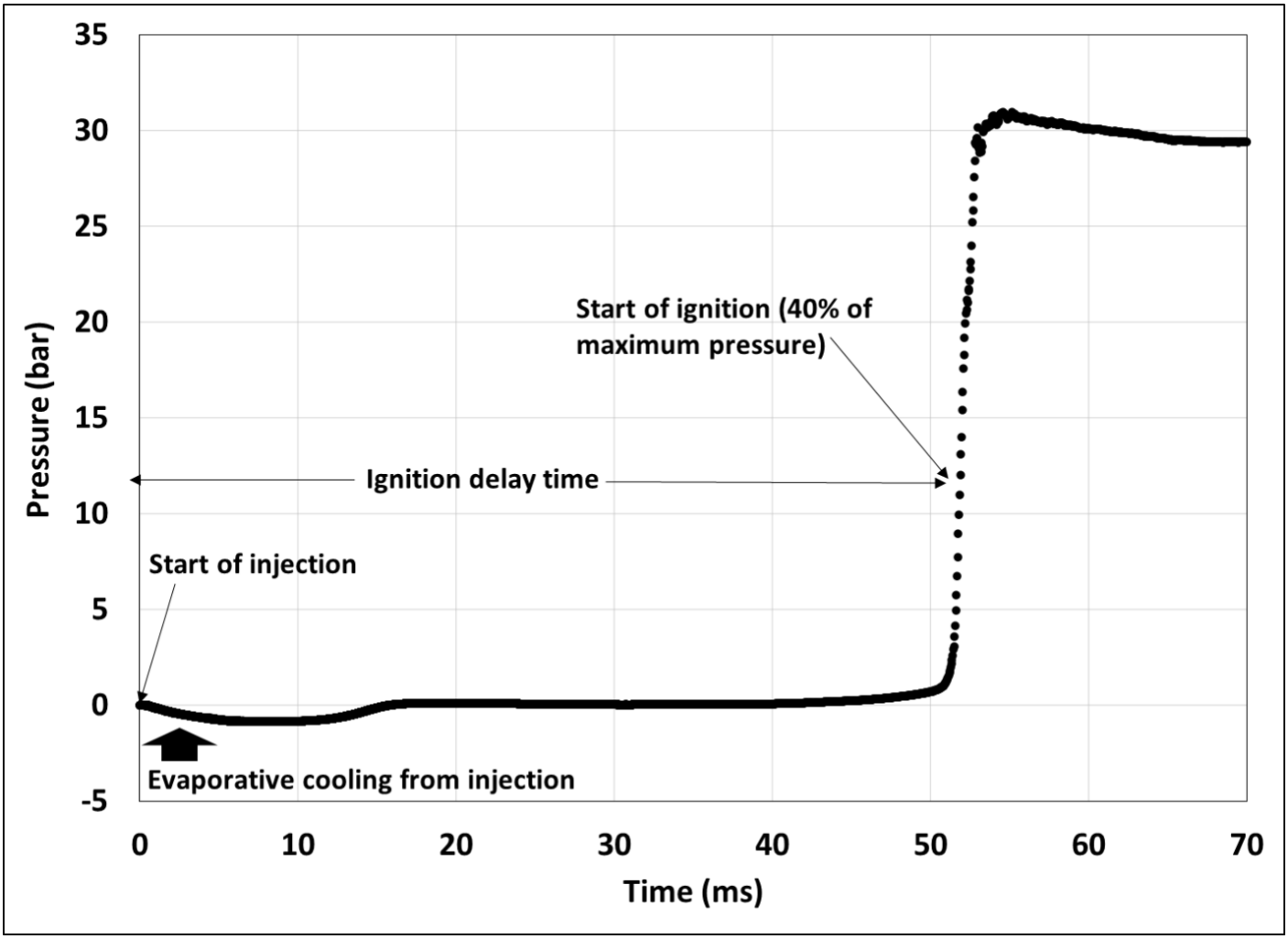

Fig. 2. Experimental pressure data example obtained from PRF-95 at 10 bar, 500°C, and 4,000-µs injection duration.

3. Results and discussion

3.1 Research octane number and octane sensitivity correlation feasibility

Even as current typical fuel chemistry combustion characterization understanding is progressing rapidly through chemical kinetic mechanism development for increasing numbers of surrogate compounds, the number of novel fuel molecules being researched outpaces chemical kinetic model development, making empirical determinations of fuel reactivity necessary. The two metrics of fuel reactivity used today, RON and MON, each typically require 500 mL of fuel, specialized equipment, and training to perform, thus presenting severe disadvantages for researchers in early-stage fuel molecule development

where available volume is limited. A fast and simple methodology was envisioned that uses measured ID times in the commercially available AFIDA CVCC device to predict RON and S, requires ≤40 mL of fuel, and is sufficiently accurate regardless of fuel chemistry.

Specific operating parameters that correlate best to RON and S needed to be identified over the wide operating range of the AFIDA, which includes a maximum of 50-bar pressure and 725°C test temperature conditions. To begin this process, three well-characterized core fuels from the U.S. Department of Energy's Co-Optimization of Fuels & Engines initiative that possess a similar RON of ~98 were chosen to probe the entire operational temperature region using 10-bar initial chamber pressure [20]. This is the highest pressure at which the injector can deliver enough fuel to achieve near-stoichiometric conditions within the combustion chamber and has shown previously to reproduce expected NTC activity in iso-octane [17]. Each custom-blended fuel contains significant differences in chemistry, providing a useful test matrix to discern ID differences regardless of chemistry. One fuel is primarily alkylate-based, providing a large amount of NTC behavior and very little S (1.4), whereas the others contain either 45% (volume) aromatics or 30% (volume) ethanol (E30) to increase S (>10) by means of differing chemistry [20]. Fig. 3 shows an Arrhenius plot of ID results at 10 bar over the test temperature range of 725°C to 400°C in 25°C increments for the initial three test fuels, along with their ASTM-measured RON, MON, and S values. For this data set, a constant injection duration was used for each fuel, leading the global fuel-air equivalence ratio (ϕ) to vary over the temperature sweep, ranging from 1.0 at the highest test temperature point of 725°C to 0.7 at the lowest test temperature point of 400°C. This occurs due to the ideal gas law, as moles of air are inversely proportional to temperature in a fixed-volume, constant-pressure system. The fuel injection duration was adjusted such that ϕ was equal for all fuels at each individual test point. Previous work with another CVCC that compared constant injected mass versus constant ϕ results in similar temperature sweeps with iso-octane/ethanol blends demonstrated that the effects of this change in ϕ within these ranges are minimal to ID [21].

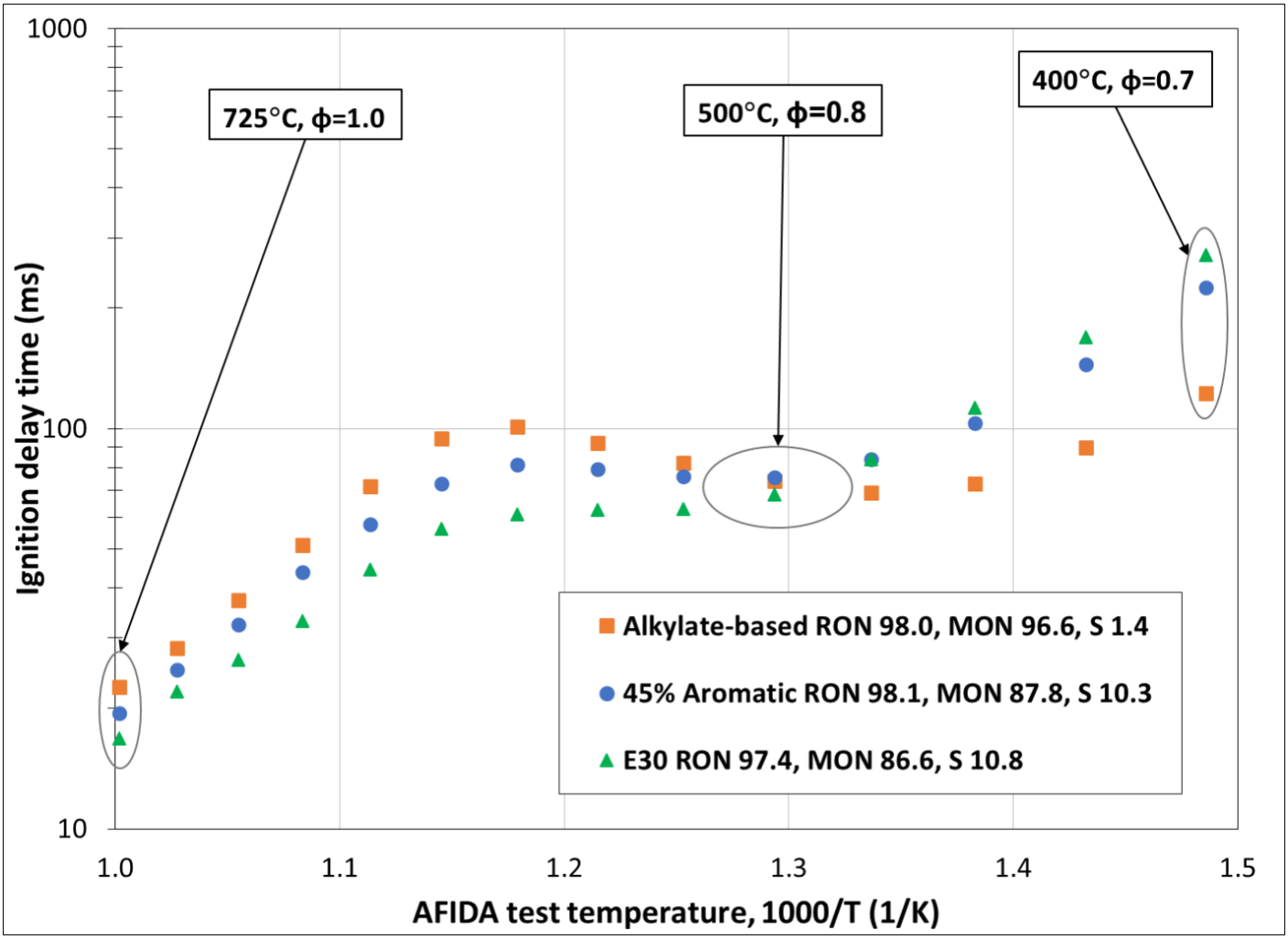

Fig. 3. Ignition delay results for three test fuels with similar RON and varying S at 10 bar, 725°C to 400°C test temperature in 25°C increments, and ϕ from 1.0 to 0.7.

Because all three fuels have a very similar RON description, identifying conditions yielding similar ID results is key for potential RON correlation. These data indicate a temperature range centered around the 500°C, 10-bar condition, for which all three fuels converge to exhibit similar ID times. Total ID times here in the range of 70–80 ms are within timescales for which the device has been previously characterized and shown to establish near-homogeneous mixtures for gasoline boiling-range fuels, meaning that the measured ID times are mostly dependent on chemical kinetics and rather unaffected by physical mixing dynamics within the device [17]. On either side of this temperature, the fuels present differing ID times, illustrating the AFIDA's ability to empirically distinguish various degrees of chemical

kinetic differences from each of the three fuel blends. Throughout the higher-temperature range from 725°C to 550°C, the E30 fuel exhibits the shortest ID times, the alkylate fuel presents the longest, and the aromatic falls in between, indicating three discrete levels of reactivity within this high-temperature window, a result that generally follows MON test results. On the lower end of the temperature sweep in the range of 475°C to 400°C, the aromatic and E30 fuels offer similar increased ID times compared to the alkylate fuel. These lower-temperature ID times exhibited by the aromatic and E30 fuels just outside of the NTC region in the AFIDA appear to correlate with the traditional S description as a measure of the temperature sensitivity of fuel reactivity. Although the test matrix is quite small, these initial results illustrate the feasibility of correlating AFIDA-based ID data to traditional CFR engine-based RON, MON, and S descriptors. The potential for a single-point RON ignition delay measurement was realized, along with a low-temperature ID slope measurement that correlates to S.

3.2 RON correlation establishment

As the optimal correlation of ID time to RON is developed, global ϕ would ideally be held constant for each fuel because this variable has the potential to affect correlation accuracy. However, doing so requires specific knowledge regarding the fuel's composition and density, which can be difficult and time-consuming to obtain. It would also require fuel injector calibration mapping, which is not feasible given the goal of characterizing fuels for which only very small quantities (~40 mL) may be available. A fixed injection duration is instead used to keep the test simple (without prior mapping of fuel mass injection rates for each fuel sample) but does result in global ϕ differences as the density and carbon, hydrogen, and oxygen composition of test fuels vary. Comparing iso-octane to ethanol illustrates an example on how global ϕ can differ between vastly compositionally different compounds. Iso-octane produces a global $\phi = 0.94$, whereas ethanol produces $\phi = 0.64$ under the developed optimal RON correlation conditions.

This RON correlation method was anchored, or "calibrated" on Fuel Set A, consisting of 31 reference fuels as shown in Table A.1, which includes PRFs and TRFs that contain 0%–40% (volume) ethanol. The correlation covers a RON range of 85–113, where the minimum-RON fuel is PRF 85 (RON 85.0) and the maximum-RON fuel is a 90% toluene, 10% ethanol blend (RON 112.8). For Fuel Set A, the following experimental test conditions were found to produce ID times that produce the greatest RON correlation potential: 4,000-µs injection duration, 1,190-bar initial fuel pressure, 10-bar air pressure, and 525°C test temperature. This test temperature is slightly greater than the temperature realized in the feasibility study (Fig. 3).

Fig. 4 shows each individual ID data point obtained from Fuel Set A, shown as both blue and orange data, in correlation to reference fuel-defined RON. A single power function regression analysis over the entire range, shown with a light gray line in Fig. 4, yields a respectable r^2 of 0.95 and a standard error (SE) of 1.8, but clearly fails to follow the data optimally throughout the entire RON region. Simply breaking the correlation curve into two discrete power functions (depicted as the blue and orange data) separated at the ignition delay time of 95 ms, which correlates to a RON of 100.6 on both power function curves (depicted in Eq. 1 and Eq. 2), increases r^2 to 0.99 and decreases SE to 1.0. Both metrics are valuable quantifications of accuracy and precision, as r^2 can be thought of as representing the "goodness of fit," representing the percentage of variance explained between one factor predicting another, whereas SE is statistically useful as 95% confidence intervals can be drawn from ±1.96 × SE. The resulting empirical equations correlating ID (in ms) to RON at 525°C and 10 bar are:

$$RON = 58.94 \times ID^{0.1174} \; for \; ID \leq 95 \; ms \quad \text{(Eq. 1)}$$

$$RON = 79.12 \times ID^{0.0527} for \; ID > 95 \; ms \quad \text{(Eq. 2)}$$

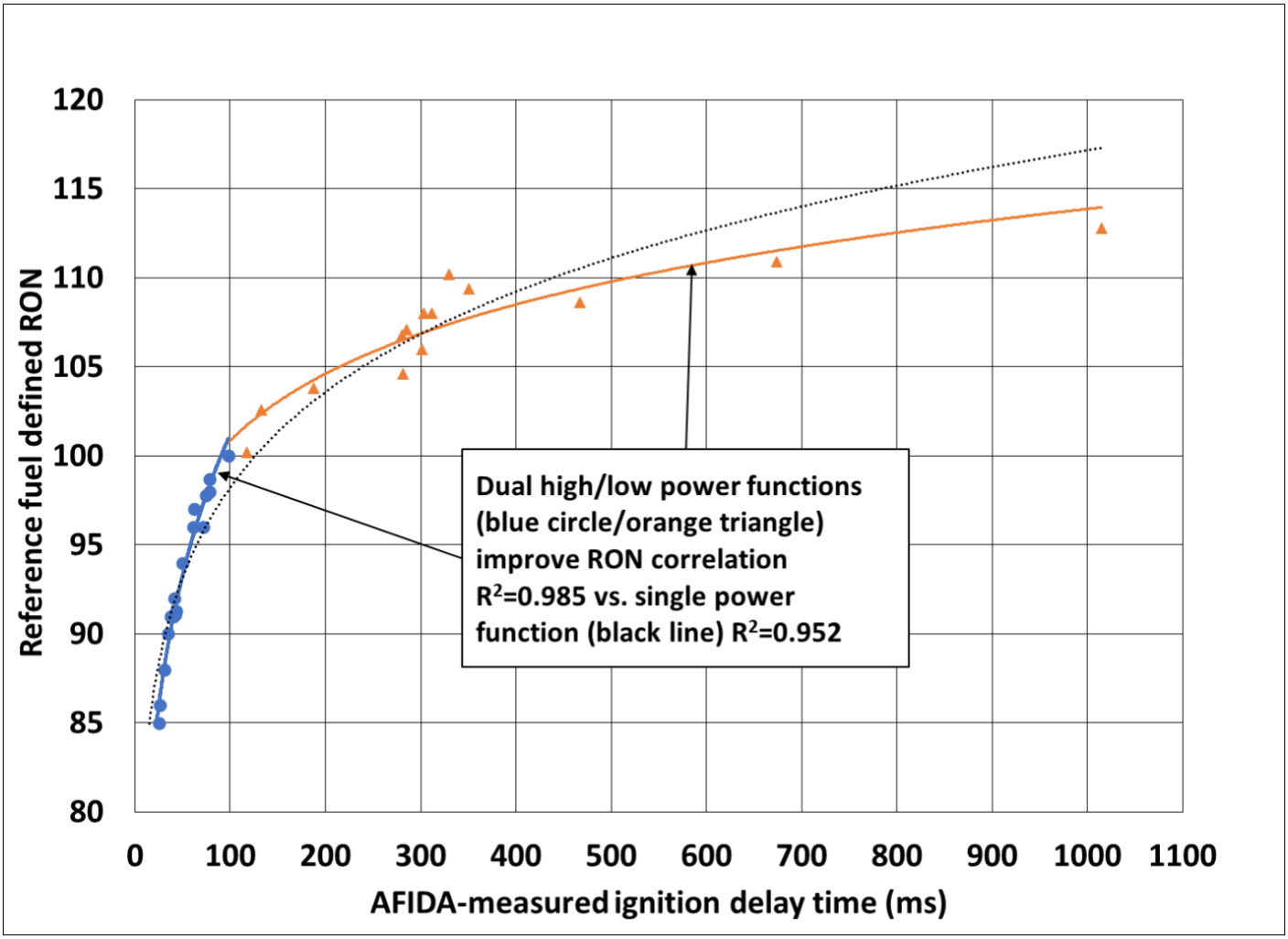

Fig. 4. Fuel Set A ID time correlation to RON at 525°C test temperature, 10-bar, and 4,000-µs injection duration conditions.

The minimum 85 RON sample corresponds to an ID time of 25 ms. Previous studies have indicated the time requirement for gasoline-range fuels to become well mixed in the combustion chamber is approximately 30 ms, a desirable condition in which the measured ID time is mostly due to fuel kinetics [17]. As ID times become shorter, the physical effects of spray breakup, evaporation, and mixing have an undesirable increasing effect on measured ID times, limiting the minimum RON range under these conditions. These physical effects combined with the correlation curve's increasing slope at shorter ID times—which results in large, predicted RON differences from small ID time changes—provides a clear lower RON predictive boundary limit under these conditions. Large increases in measured ID time

produce very small increases in RON throughout the high-RON correlation curve, as the 113 RON point at the high end of the RON correlation corresponds to an ignition delay time of 1,015 ms. Beyond this point, fuels with increasing RON do not ignite repeatably and may not ignite at all. The clear implications from these observations are that lower temperatures and pressures (to increase ID times) would be required to accurately characterize fuels with RON < 85, whereas higher temperatures and pressures (to decrease ID times) are necessary for fuels with RON > 113, however, any potential new temperature and pressure testing conditions will affect NTC activity and would need to be considered. Iso-octane ID times averaging ~98 ms were measured repeatedly throughout methodology development, displaying a standard deviation of 2.27 ms over 17 samples, which is typical across experiments with similar ID times. Experiments exhibiting shorter ID times tend to produce less standard deviation, while experiments leading to longer ID times produce greater standard deviation. The shortest 25 ms ID time observed from PRF 85 displayed a 0.22 standard deviation between 12 injections, while a significantly longer ID time of 303 ms observed from ethanol displayed standard deviation of 11.95.

3.3 RON prediction validation results

Methodology validation was performed on Fuel Set B listed in Table A.2, consisting of five pump gasoline samples, five high-octane surrogate blends, and 92 other research fuels that have been previously well characterized for composition and reactivity. The pump gasoline samples include three samples of varying antiknock index that contain ethanol, one without ethanol, and one racing fuel. The five high-octane surrogate blends, comprising triptane, cyclopentane, diisobutylene, and ethylbenzene, were supplied and analyzed for RON and MON by Petrobras. The 92 research fuels are made up from five separate surrogate base fuels, designed to have similar reactivity as defined by RON and MON but spanning significantly different chemistries for which the major component is either paraffin, iso-paraffin, naphthene, aromatic, or olefin. The surrogate compounds used to prepare these base fuels consisted of n-pentane, n-heptane, iso-pentane, 2,2,4-trimethylpentane, 1-hexene, 2,4,4-trimethyl-1-

pentane, cyclopentane, toluene, and 1,2,4-trimethylbenzene. Individual additives including ethanol, isobutanol, diisobutylene, methyl acetate, 3-pentanone, and 2-methylfuran were then blended into the base fuels at 10%–30% volumetric levels, adding chemistry spanning alcohol, olefin, ketone, and furan groups to the different base fuel compositions. This unique combination of base fuel and additive chemistry, prepared as a result of the Co-Optimization of Fuels & Engines initiative, provided a very challenging matrix over which to interrogate the utility and robustness of the empirical correlation methodology.

Fig. 5 displays a parity plot of all data broken into the 10 relevant categories, with the AFIDA-predicted RON shown on the y-axis using the dual high-/low-power function correlation described in Eq. 1 and Eq. 2 versus the CFR-measured RON on the x-axis. The average total error for Fuel Set B is −1.1%, calculated by averaging each individual error. This overall negative bias describes the methodology as generally producing a slight underprediction of RON, visually illustrated by the majority of data points falling slightly beneath the ideal correlation dotted line. Because positive and negative errors can offset, another metric called absolute total error was calculated to be 1.6%, the difference here being that all individual absolute error measurements were averaged, providing a better indication of overall accuracy of the AFIDA-predicted RON value vs. the CFR-measured value. The largest individual positive and negative error obtained was 2.2% and −4.3% respectively. Measured r^2 for Fuel Set B is 0.94 and SE is 1.3, calculated using all data points.

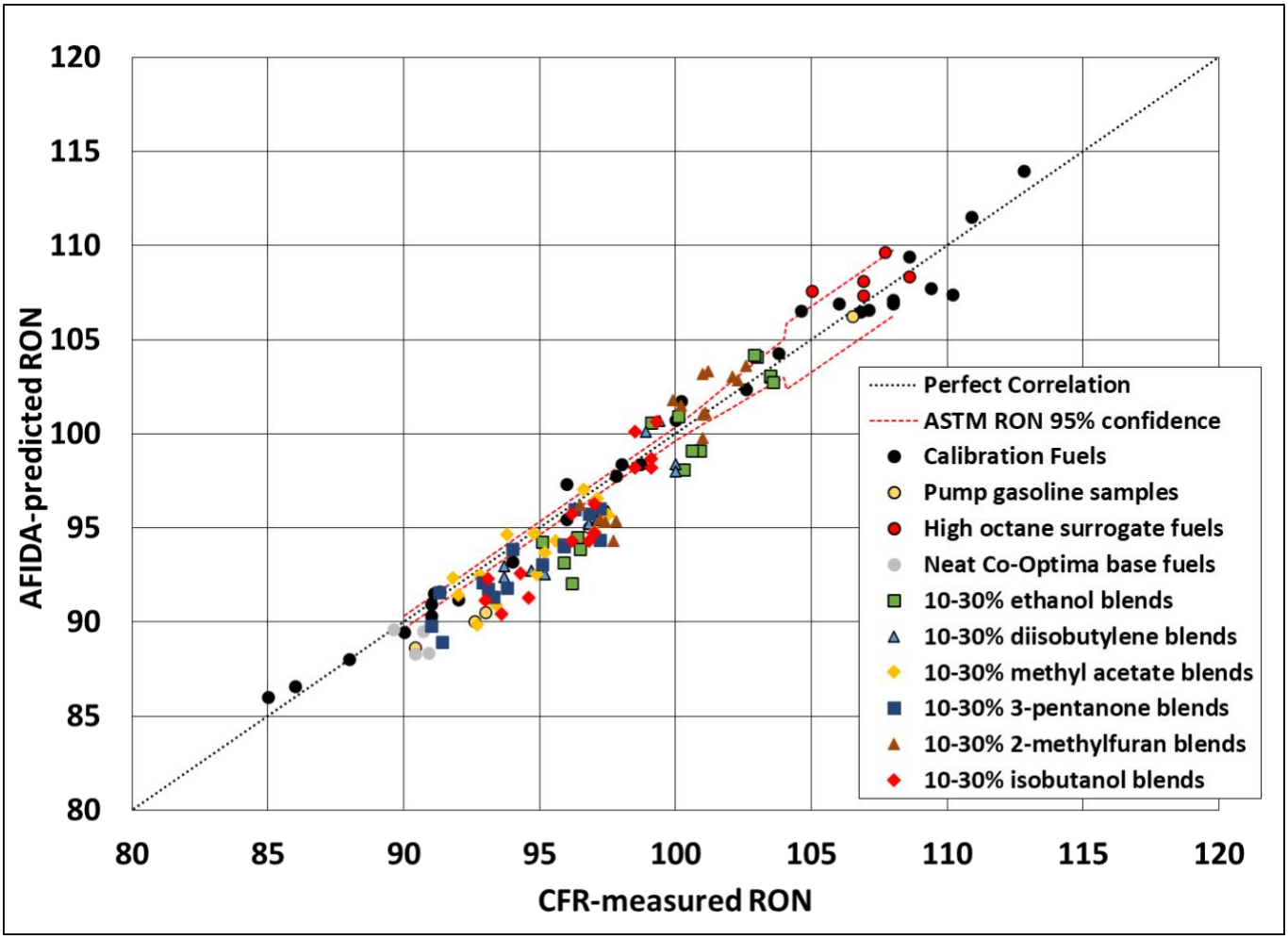

Fig. 5. Parity plot showing AFIDA-predicted RON (y-axis) versus CFR-measured RON (x-axis) of all samples showing ideal correlation (black dotted) and CFR-measured RON reproducibility bands (red dotted).

Table 1 shows detailed error comparisons between categories. Predictably, the reference fuels "calibration" group provides the best overall accuracy, but it is notable how consistent the various error metrics are across all the very different categories. The most surprising trend is observed accuracy improvements as single-component blend levels increase from 10% to 30%, which may be arbitrary, but does provide clear evidence that the methodology is not limited to typical hydrocarbon-based chemistry. Fuel-air equivalence ratio differences introduced as a result of stoichiometric shifts due to various fuel chemistries, a concern because of the use of a fixed injection duration (volume), did not lead to any measurable accuracy differences between categories. Considering that the ASTM D2699 lists

the reproducibility of RON in the range of 90–100 RON at 0.7, meaning two independent laboratories would be likely to produce results within 0.7 units with 95% confidence [3], the AFIDA RON predictions over the same range display increased SE. Reproducibility numbers for the ASTM method increase as RON increases, reaching 3.5 above 104 RON, displayed as red dotted lines in Fig. 5 [3]. The AFIDA-based methodology may be more accurate and precise than the ASTM method for describing RON > 104, whereas the ASTM method shows increased accuracy and precision when RON < 100. The empirical RON correlation to ID time developed here uses only one test condition (525°C, 10 bar), but the resulting validation appears to be valuable. Adding more test conditions to further improve accuracy would require a larger fuel volume, conflicting with one of the key benefits of this methodology.

Table 1. RON correlation error analysis between validation groupings.

	Avg. Total		**Avg. Absolute**		**Max. positive error**		**Max. negative error**	
Category	**Difference**	**%**	**Difference**	**%**	**Difference**	**%**	**Difference**	**%**
Reference “calibration” fuels	0.0	0.0%	0.8	0.8%	1.9	1.8%	−2.8	−2.5%
Pump gasolines	−1.8	−1.9%	1.8	1.9%	n/a	n/a	−2.6	−2.8%
High-octane surrogate fuels	1.2	1.1%	1.3	1.2%	2.6	2.5%	−0.2	−0.2%
Neat base fuels	−1.5	−1.6%	1.5	1.6%	n/a	n/a	−2.5	−2.8%
10%–30% ethanol blends	−1.0	−1.0%	1.6	1.6%	1.5	1.5%	−4.1	−4.3%
10%–30% diisobutylene blends	−1.2	−1.2%	1.6	1.6%	1.3	1.3%	−2.7	−2.8%
10%–30% methyl acetate blends	−1.0	−1.1%	1.3	1.4%	0.9	0.9%	−2.9	−3.1%
10%–30% 3-pentanone blends	−1.4	−1.5%	1.4	1.5%	0.3	0.3%	−2.9	−2.9%
10%–30% 2-methylfuran blends	−0.1	−0.1%	1.4	1.4%	2.2	2.2%	−3.4	−3.5%
10%–30% isobutanol blends	−1.2	−1.2%	1.6	1.6%	1.6	1.6%	−3.3	−3.5%
10% additive blends	−1.8	−1.9%	1.8	1.9%	0.6	0.6%	−4.1	−4.3%
20% additive blends	−0.9	−1.0%	1.4	1.4%	1.9	1.9%	−2.5	−2.6%
30% additive blends	−0.1	−0.2%	1.2	1.2%	2.2	2.2%	−2.9	−2.9%

This validation effort demonstrates the robustness of this testing methodology irrespective of fuel chemistry. Although not flawless, this correlation could prove useful to those researchers seeking

quantitative RON characterization without being imposed with sample volume and time requirements of traditional methodology. Other experimental temperature and pressure conditions may be well suited to characterize autoignition resistance for specific engine operating conditions employed in modern and future engines for which RON and MON descriptors alone fail, making this test methodology, which is faster, easier, and requires less volume than traditional methods, important for the future characterization of fuels.

3.4 Octane sensitivity correlation establishment

Combined with RON, S is a very important fuel characterization metric relating fuel autoignition resistance to modern engines, traditionally captured by measuring a fuel's RON and MON and calculating the difference between them. Attempts to correlate AFIDA ID time results to MON were somewhat successful, but not adequate to be quantitatively relevant. The measured ID times for the 30% ethanol and 45% aromatic fuels with similar sensitivity, shown in Fig. 3, indicate sensitivity correlation with the slope of the ID times measured external to the NTC region on the lower-temperature side. Kineticists have successfully used the slope from chemistry-based ID time calculations though the NTC region to correlate to S [10], and the approach here is similar but relies on AFIDA-based empirical ID time measurements at two temperature conditions, from which a slope is determined and used to predict S. It is recognized that other fuel properties such as heat of vaporization and flame speed may affect S, but the assumption is that measurable chemical kinetics is the most significant contributing factor. It is recognized that the use of a fixed injection duration results in more globally lean stoichiometry for oxygenated fuels, and since stoichiometry affects NTC chemistry, there is a trade-off in accuracy for comparing fuel NTC activity by using a quick test requiring a small fuel quantity versus holding stoichiometry constant.

348 Fig. 6 shows ID plots of four fuels that exhibit a similar 91 RON and present varying levels of S, ranging
349 from 0–7.6. Fuels with increasing S produce a clear trend of increasing slope of ID time at temperatures
350 below 475°C. Optimum experimental conditions that correlate IDT slope to S were found to occur
351 between 425°C–475°C test temperatures at 10 bar, using a fixed injection duration of 4,000 µs.

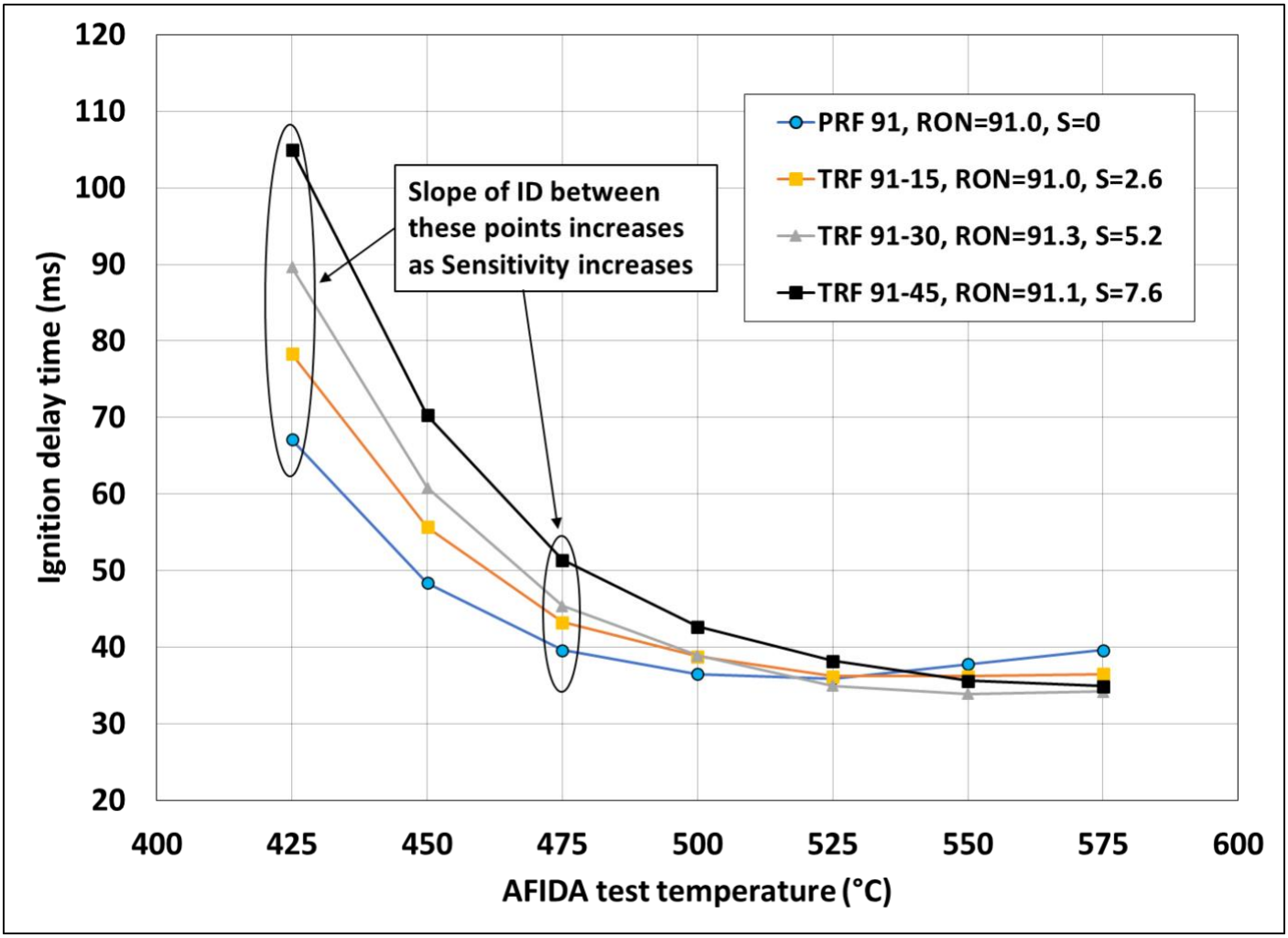

352

353 Fig. 6. Sensitivity effects on ID time over AFIDA test temperature for fuels with similar RON at 10 bar,
354 4,000-µs injection duration conditions.

355 Fuel Set A was used to derive the empirical correlation of ID time slope to S, similar to the RON
356 correlation establishment in Section 3.2, thereby "calibrating" or anchoring the methodology on
357 reference fuels in an attempt to create the most robust applicability. The four highest-S samples did not
358 ignite at the two test temperatures and were not included. Fig. 7 displays the empirical correlation (Eq.

3) for S, established using a natural logarithmic function from the slope of ID (in ms) over the 50°C temperature difference. The resulting correlation yields an r^2 of 0.97 and SE of 0.69 for all samples in Fuel Set A. Very unreactive samples that present a slope beyond the reach of the correlation curve (>2.45) are reported as having S > 12 and are not included in r^2 or SE calculations, whereas samples predicted to have a negative S are represented as 0 and are included in r^2 and SE calculations. Sensitivity cannot be predicted for any sample which displays a negative slope.

$$S = 7.79 \times \ln((ID@425℃ - ID@475℃)/25) + 5.00 \quad \text{(Eq. 3)}$$

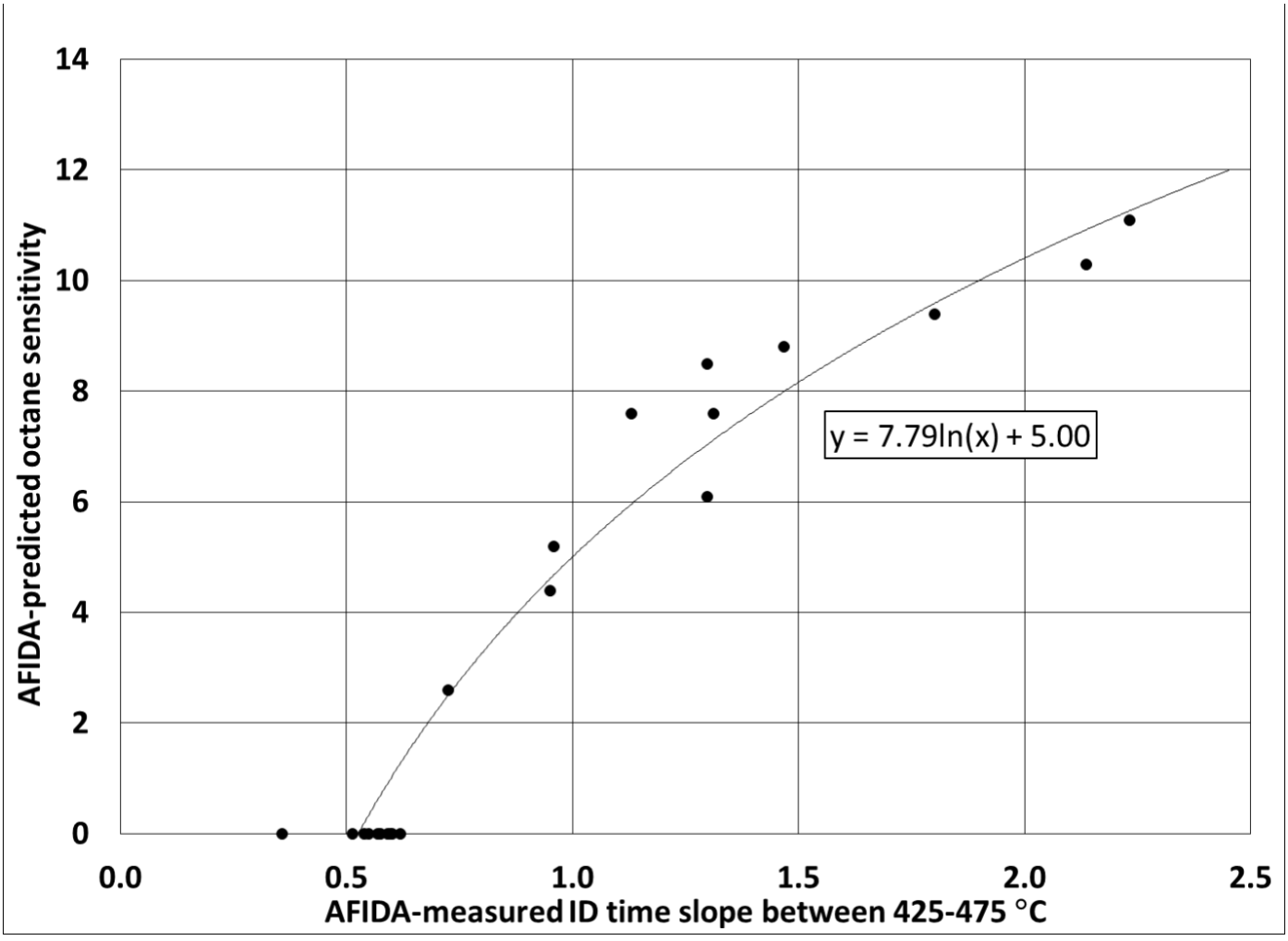

Fig. 7. ID time slope correlation to S between 425°C and 475°C test temperatures, 10-bar, 4,000-µs injection duration conditions.

3.5 Octane sensitivity correlation validation results

Octane sensitivity methodology validation was performed on the same Fuel Set B used for RON validation, and results are plotted on a parity plot shown in Fig. 8, where the AFIDA-predicted S is plotted on the y-axis versus the ASTM CFR-measured S plotted on the x-axis. The dotted line, representing a perfect correlation, extends to an S of 12, at which point the methodology yields a result of S > 12, represented graphically by placing the point along the y-axis (AFIDA-predicted S) at 12.5, slightly removed from the quantitative predictions up to 12.0. Fuel Set B presents average total error of −1.7 units (−20.0%), which indicates an underprediction of S overall, graphically observed as most data points fall beneath the ideal correlation line. Absolute total error of 1.9 units (22.7%), r^2 of 0.48, SE of 1.9, and maximum positive and negative errors of 2.2 units (51%) and −7.4 units (−88%), respectively, indicate large uncertainty at predicting S, but further analysis indicates the uncertainty is not evenly spread throughout the data. Although none of the S > 12 predictions were used in the error analysis or calculation of r^2 or SE, that portion of the methodology is quite valuable, as all 13 predictions are accurate in predicting high S, a very desirable fuel property.

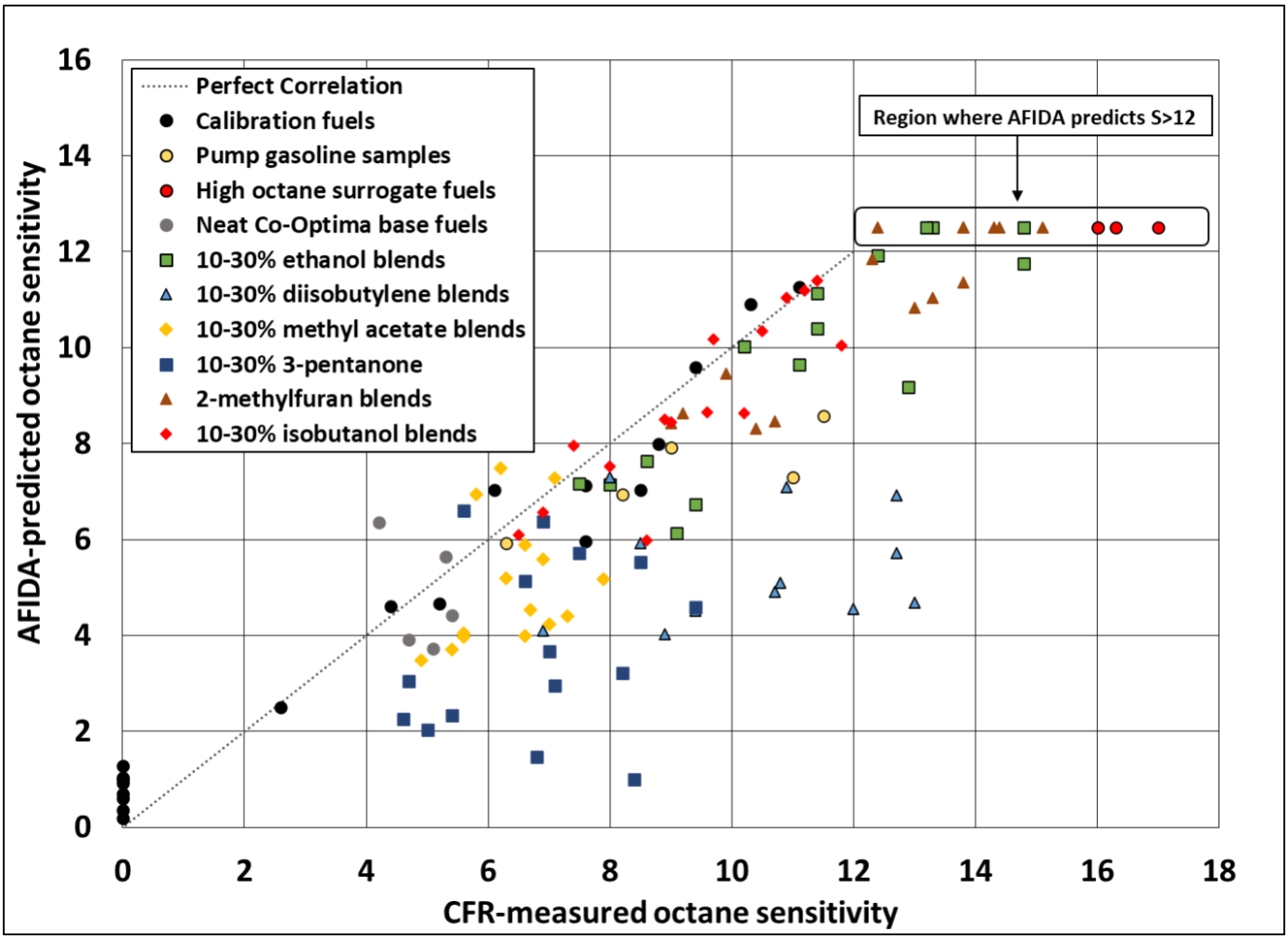

Fig. 8. Parity plot showing AFIDA-predicted S (y-axis) versus CFR-measured S (x-axis) of all samples.

Unlike the RON correlation, AFIDA S predictive accuracy throughout the range and within categories yields different results, as indicated by Table 2. For most categories (excluding diisobutylene and 3-pentanone blends), the correlation performs well at predicting S, with maximum error range of 2.2 and −3.7, and overall absolute error averaging 1.3 units. Diisobutylene and 3-pentanone are clear outliers as S is severely underpredicted by ~45%; removing them from the regression analysis yields significant improvements in r^2 from 0.48 to 0.78 and SE from 1.9 to 1.2. Those two compounds result in S predictive error increasing as blend percentage increases, unlike the RON correlation. The reason for the prediction problems arising from these two additive compounds is not clearly understood as ID time

394 measurements at only three conditions were performed, and further understanding of the kinetic
395 behavior of these blends requires a more detailed analysis of the kinetics over the entire NTC
396 temperature region, which was not performed in this study. Since octane sensitivity is coupled with NTC
397 chemistry, a more detailed understanding of NTC activity, established by measuring ID times at
398 additional temperature conditions, would likely improve sensitivity predictions, but would also require
399 the use of additional fuel.

400 Table 2. Octane sensitivity correlation error analysis between validation groupings.

	Avg. Total		Avg. Absolute		Max. positive error		Max. negative error	
Category	**Difference**	**%**	**Difference**	**%**	**Difference**	**%**	**Difference**	**%**
Calibration fuels	0.0	0%	0.8	n/a	1.3	n/a	−3.0	n/a
Pump gasolines	−1.9	−18.5%	1.9	18.5%	n/a	n/a	−3.7	−33.7%
High-octane surrogate fuels	n/a	n/a	n/a	n/a	n/a	n/a	n/a	n/a
Neat base fuels	−0.1	−0.8%	1.1	23.9%	2.2	51.2%	−1.4	−26.9%
10%–30% ethanol blends	−1.5	−13.9%	1.5	13.9%	n/a	n/a	−3.0	−32.7%
10%–30% diisobutylene blends	−5.0	−46.2%	5.0	46.2%	n/a	n/a	−8.3	−64.0%
10%–30% methyl acetate blends	−1.3	−20.5%	1.7	26.3%	1.3	20.9%	−2.9	−39.8%
10%–30% 3-pentanone blends	−3.1	−43.8%	3.2	46.2%	1.0	18.0%	−7.4	−88.1%
10%–30% 2-methylfuran blends	−1.5	−12.5%	1.5	12.5%	n/a	n/a	−2.3	−20.8%
10%–30% isobutanol blends	−0.5	−5.8%	0.7	7.7%	0.6	7.5%	−2.6	−30.3%
10% additive blends	−1.5	−19.5%	1.6	22.6%	1.1	19.8%	−4.1	−58.3%
20% additive blends	−2.0	−22.9%	2.2	24.7%	1.3	20.9%	−5.0	−60.8%
30% additive blends	−3.3	−34.2%	3.3	34.3%	0.1	1.3%	−7.4	−88.1%

401

402 Two chemistries causing S correlative problems involving a ketone and a specific olefin were identified
403 and provide fuel researchers guidelines for this S correlation methodology applicability, which, unlike
404 RON, does not appear to be universally applicable. One base fuel incorporates maximum olefin
405 composition, indicating olefins in general are not causing major S correlative issues. It is unknown
406 whether ketone additive chemistry in general is a problem or if the poor correlation is related to the

specific ketone tested. For most combinations of base fuel and chemistry additive, S correlation based on measured ID time slope provides a reasonable estimation for the fuel property and results in almost no error in overpredicting S, especially true when predicted S > 7. Because high-S fuels are typically desirable, understanding this methodology error becomes valuable as strong confidence exists that a high-S AFIDA prediction is likely a minimum number.

Octane sensitivity resulting from ethanol addition has been widely researched and the ability of engine technologies to utilize these kinetic affects are well documented, but this is not the case for these new additive chemistries. The AFIDA low-temperature kinetic approach correlates well with most chemistries, including ethanol addition, setting up an interesting question as to whether the ASTM engine-based methods contain any chemistry bias. Further engine research using nontraditional fuel chemistry is required to validate whether the ASTM methods themselves are universally applicable with regards to chemistry at producing RON, MON, and S values that are useful at predicting advantageous fuel properties which can be utilized in modern engines.

Conclusion

A novel methodology is presented that correlates ID time measurements obtained using the commercially available AFIDA constant-volume combustion chamber to currently established ASTM fuel autoignition metrics, including RON and S. Advantages over traditional CFR engine-based testing methodologies include significantly smaller sample volume requirements (40 mL vs. 1 L), faster turnaround time (1 hour vs. 24+ hours), and overall experimental simplicity.

An optimized empirical RON correlation was developed that correlates a single ID time measurement to RON for reference fuels that define the RON scale with a resulting r^2 of 0.99 and SE of 1.0, achieved using the following experimental conditions: 10 bar, 4,000-µs injection duration, and 525°C test temperature. The RON correlation, effective over the range of 85–113 RON, was validated over a

complex matrix of 102 fuels designed to test the robustness of the methodology against both traditional and nontraditional fuel chemistry, which included pump gasoline samples, high-octane surrogate blends, five base fuels comprising different majority chemistries, and six 10%–30% RON-enhancing additive compounds containing various functional groups including ethanol, isobutanol, diisobutylene, methyl acetate, 3-pentanone, and 2-methylfuran. This extensive validation effort produced a RON correlation with r^2 of 0.94 and SE of 1.3, with error distributed equally among all various groupings, highlighting the robust applicability of this methodology.

Octane sensitivity, traditionally calculated from the difference between the RON and MON, was demonstrated to correlate well with ID time slope measurements obtained in the low-temperature region below 475°C, as fuels with higher S show an increasing ID time slope over fuels with lower S. A methodology was optimized that correlates the slope of the ID time measured between 425°C and 475°C test temperatures to S of reference fuels, with a resulting r^2 of 0.97 and SE of 0.69 using 10-bar 4,000-µs duration experimental conditions, with the concession that fuels with S > 12 are indistinguishable. This methodology was then validated over the same complex fuel matrix used for RON validation, indicating the two additives 3-pentanone and diisobutylene displayed poor S correlation compared to the rest of the matrix, which resulted in r^2 of 0.78 and SE = 1.2 without their inclusion. AFIDA-based S predictions, although not entirely accurate, can identify desirable high-octane-sensitive fuels.

Not only are AFIDA fuel ignition delay measurements for gasoline-range fuels at conditions that correlate well to RON and S useful, but potential exists to develop new metrics that may more fully describe fuel autoignition quality over a wide variety of operating conditions, which may correlate better to modern engines using advanced engine operating modes for which RON, MON, and S alone are inadequate.

Acknowledgements

This work was authored by the National Renewable Energy Laboratory, operated by Alliance for Sustainable Energy, LLC, for the U.S. Department of Energy (DOE) under Contract No. DE-AC36-08GO28308. Funding was provided by the U.S. Department of Energy's Office of Energy Efficiency and Renewable Energy, Vehicle Technologies Office. The views expressed in the article do not necessarily represent the views of the DOE or the U.S. Government. The U.S. Government retains and the publisher, by accepting the article for publication, acknowledges that the U.S. Government retains a nonexclusive, paid-up, irrevocable, worldwide license to publish or reproduce the published form of this work, or allow others to do so, for U.S. Government purposes.

This research was conducted as part of the Co-Optimization of Fuels & Engines (Co-Optima) project. Co-Optima is a collaborative project of several national laboratories initiated to simultaneously accelerate the introduction of affordable, scalable, and sustainable biofuels and high-efficiency, low-emission vehicle engines. The authors thank program manager Kevin Stork at the DOE Vehicle Technologies Office for supporting this research under the Co-Optima project.

The authors would like to thank Gina Fioroni at the National Renewable Energy Laboratory and Matthew McNenly at Lawrence Livermore National Laboratory for sharing fuel samples and data in collaboration under Co-Optima. The authors would also like to thank Ana Carolina Bontorin and colleagues at Petrobras Research and Development Center for sharing fuel samples used in this research.

Appendix

Table A.1 Fuel Set A (31 samples) showing defined or previously measured RON, MON, and S values [22].

Fuel ID	RON	MON	S	Composition (volume fraction)
PRF 85	85.0	85.0	0	85% iso-octane, 15% n-heptane
PRF 86	86.0	86.0	0	86% iso-octane, 14% n-heptane
PRF 88	88.0	88.0	0	88% iso-octane, 12% n-heptane

PRF 90	90.0	90.0	0	90% iso-octane, 10% n-heptane
PRF 91	91.0	91.0	0	91% iso-octane, 9% n-heptane
TRF 91-15	91.0	88.4	2.6	72.6% iso-octane, 12.4% n-heptane, 15% toluene
TRF 91-45	91.1	83.5	7.6	34.7% iso-octane, 20.3% n-heptane, 45% toluene
TRF 91-30	91.3	86.1	5.2	53.2% iso-octane, 17% n-heptane, 29.8% toluene
PRF 92	92.0	92.0	0	92% iso-octane, 8% n-heptane
PRF 94	94.0	94.0	0	94% iso-octane, 6% n-heptane
PRF 96	96.0	96.0	0	96% iso-octane, 4% n-heptane
TRF 91-45-E10	96.0	87.2	8.8	90% TRF 91-45, 10% ethanol
TRF 91-30-E10	97.0	89.4	7.6	90% TRF 91-30, 10% ethanol
TRF 91-15-E10	97.8	91.7	6.1	90% TRF 91-15, 10% ethanol
PRF 98	98.0	98.0	0	98% iso-octane, 2% n-heptane
PRF 91-E10	98.7	94.3	4.4	90% PRF 91, 10% ethanol
PRF 100	100.0	100.0	0	100% iso-octane
TRF 91-45-E20	100.2	89.1	11.1	80% TRF 91-45, 20% ethanol
TRF 91-15-E20	102.6	93.2	9.4	80% TRF 91-15, 20% ethanol
PRF 91-20	103.8	95.3	8.5	80% PRF 91, 20% ethanol
TRF 91-45-E40	104.6	90.9	13.7	60% TRF 91-45, 40% ethanol
TRF 91-30-E40	106.0	92.1	13.9	60% TRF 91-30, 40% ethanol
PRF 100-E10	106.8	99.9	6.9	90% iso-octane, 10% ethanol
TRF 91-15-E40	107.1	93.6	13.5	60% TRF 91-15, 40% ethanol
PRF 91-E40	108.0	94.5	13.5	60% PRF 91, 40% ethanol
E100	108.0	90.7	17.3	100% ethanol
Tol-E40	108.6	93.3	15.3	60% toluene, 40% ethanol
PRF 100-E20	109.4	99.1	10.3	80% iso-octane, 20% ethanol
PRF 100-E40	110.2	95.9	14.3	80% iso-octane, 20% ethanol
Tol-E20	110.9	97.0	13.9	80% toluene, 20% ethanol
Tol-E10	112.8	101.0	11.8	90% toluene, 10% ethanol

473

474 Table A.2 Fuel Set B (102 samples) showing ASTM-measured RON, MON, and S values.

Fuel ID	**RON**	**MON**	**S**	**Composition**
Neat (max olefin base – O)	90.9	85.5	5.4	Olefinic base fuel
Neat (max naphthene base – N)	89.6	85.4	4.2	Naphthene base fuel
Neat (max aromatic base – A)	90.4	85.3	5.1	Aromatic base fuel
Neat (max paraffin base – P)	90.7	85.4	5.3	Paraffinic base fuel
Neat (max iso-paraffin base – I)	90.5	85.8	4.7	Iso-paraffinic base fuel

10% ethanol in O	96.5	87.1	9.4	90% max olefin, 10% ethanol
20% ethanol in O	100.9	88.0	12.9	80% max olefin, 20% ethanol
30% ethanol in O	103.5	88.7	14.8	70% max olefin, 30% ethanol
10% ethanol in N	95.1	86.5	8.6	90% max naphthene, 10% ethanol
20% ethanol in N	99.1	87.7	11.4	80% max naphthene, 20% ethanol
30% ethanol in N	103.0	88.2	14.8	70% max naphthene, 30% ethanol
10% ethanol in A	95.9	87.9	8.0	90% max aromatic, 10% ethanol
20% ethanol in A	100.6	89.5	11.1	80% max aromatic, 20% ethanol
30% ethanol in A	103.5	90.2	13.3	70% max aromatic, 30% ethanol
10% ethanol in P	96.4	87.3	9.1	90% max paraffin, 10% ethanol
20% ethanol in P	100.1	88.7	11.4	80% max paraffin, 20% ethanol
30% ethanol in P	102.9	90.5	12.4	70% max paraffin, 30% ethanol
10% ethanol in I	96.2	88.7	7.5	90% max iso-paraffin, 10% ethanol
20% ethanol in I	100.3	90.1	10.2	80% max iso-paraffin, 20% ethanol
30% ethanol in I	103.6	90.4	13.2	70% max iso-paraffin, 30% ethanol

10% diisobutylene in O	95.2	86.3	8.9	90% max olefin, 10% diisobutylene
20% diisobutylene in O	97.5	86.8	10.7	80% max olefin, 20% diisobutylene
30% diisobutylene in O	100.0	87.0	13.0	70% max olefin, 30% diisobutylene
10% diisobutylene in N	93.7	85.7	8.0	90% max naphthene, 10% diisobutylene
20% diisobutylene in N	96.8	85.9	10.9	80% max naphthene, 20% diisobutylene
30% diisobutylene in N	98.9	86.2	12.7	70% max naphthene, 30% diisobutylene
10% diisobutylene in A	93.7	86.8	6.9	90% max aromatic, 10% diisobutylene
20% diisobutylene in A	97.1	87.7	9.4	80% max aromatic, 20% diisobutylene
30% diisobutylene in A	100.0	88.0	12.0	70% max aromatic, 30% diisobutylene
10% diisobutylene in P	94.7	86.2	8.5	90% max paraffin, 10% diisobutylene
20% diisobutylene in P	97.4	86.6	10.8	80% max paraffin, 20% diisobutylene
30% diisobutylene in P	99.4	86.7	12.7	70% max paraffin, 30% diisobutylene

10% methyl acetate in O	93.4	86.8	6.6	90% max olefin, 10% methyl acetate
20% methyl acetate in O	95.6	88.3	7.3	80% max olefin, 20% methyl acetate
30% methyl acetate in O	97.5	89.6	7.9	70% max olefin, 30% methyl acetate
10% methyl acetate in N	91.8	86.0	5.8	90% max naphthene, 10% methyl acetate
20% methyl acetate in N	93.8	87.6	6.2	80% max naphthene, 20% methyl acetate
30% methyl acetate in N	96.1	89.0	7.1	70% max naphthene, 30% methyl acetate
10% methyl acetate in A	92.0	86.6	5.4	90% max aromatic, 10% methyl acetate
20% methyl acetate in A	95.2	88.2	7.0	80% max aromatic, 20% methyl acetate
30% methyl acetate in A	97.1	90.2	6.9	70% max aromatic, 30% methyl acetate

10% methyl acetate in P	92.8	86.5	6.3	90% max paraffin, 10% methyl acetate
20% methyl acetate in P	94.8	88.2	6.6	80% max paraffin, 20% methyl acetate
30% methyl acetate in P	96.6	89.9	6.7	70% max paraffin, 30% methyl acetate
10% methyl acetate in I	92.7	87.8	4.9	90% max iso-paraffin, 10% methyl acetate
20% methyl acetate in I	94.9	89.3	5.6	80% max iso-paraffin, 20% methyl acetate
30% methyl acetate in I	97.0	91.4	5.6	70% max iso-paraffin, 30% methyl acetate
10% 3-pentanone in O	93.8	86.7	7.1	90% max olefin, 10% 3-pentanone
20% 3-pentanone in O	95.9	87.7	8.2	80% max olefin, 20% 3-pentanone
30% 3-pentanone in O	96.8	88.4	8.4	70% max olefin, 30% 3-pentanone
10% 3-pentanone in N	91.3	85.7	5.6	90% max naphthene, 10% 3-pentanone
20% 3-pentanone in N	94.0	87.1	6.9	80% max naphthene, 20% 3-pentanone
30% 3-pentanone in N	96.3	87.8	8.5	70% max naphthene, 30% 3-pentanone
10% 3-pentanone in A	91.0	86.3	4.7	90% max aromatic, 10% 3-pentanone
20% 3-pentanone in A	93.1	87.7	5.4	80% max aromatic, 20% 3-pentanone
30% 3-pentanone in A	95.9	89.1	6.8	70% max aromatic, 30% 3-pentanone
10% 3-pentanone in P	92.9	86.3	6.6	90% max paraffin, 10% 3-pentanone
20% 3-pentanone in P	95.1	87.6	7.5	80% max paraffin, 20% 3-pentanone
30% 3-pentanone in P	97.2	87.8	9.4	70% max paraffin, 30% 3-pentanone
10% 3-pentanone in I	91.4	86.8	4.6	90% max iso-paraffin, 10% 3-pentanone
20% 3-pentanone in I	93.3	88.3	5.0	80% max iso-paraffin, 20% 3-pentanone
30% 3-pentanone in I	97.2	90.2	7.0	70% max iso-paraffin, 30% 3-pentanone
10% 2-methylfuran in O	97.8	87.1	10.7	90% max olefin, 10% 2-methylfuran
20% 2-methylfuran in O	101.0	87.2	13.8	80% max olefin, 20% 2-methylfuran
30% 2-methylfuran in O	102.1	87.0	15.1	70% max olefin, 30% 2-methylfuran
10% 2-methylfuran in N	96.5	86.6	9.9	90% max naphthene, 10% 2-methylfuran
20% 2-methylfuran in N	100.2	86.9	13.3	80% max naphthene, 20% 2-methylfuran
30% 2-methylfuran in N	101.0	86.7	14.3	70% max naphthene, 30% 2-methylfuran
10% 2-methylfuran in A	97.2	88.0	9.2	90% max aromatic, 10% 2-methylfuran
20% 2-methylfuran in A	101.1	88.7	12.4	80% max aromatic, 20% 2-methylfuran
30% 2-methylfuran in A	102.6	88.8	13.8	70% max aromatic, 30% 2-methylfuran
10% 2-methylfuran in P	97.4	87.0	10.4	90% max paraffin, 10% 2-methylfuran
20% 2-methylfuran in P	99.9	86.9	13.0	80% max paraffin, 20% 2-methylfuran
30% 2-methylfuran in P	101.2	86.8	14.4	70% max paraffin, 30% 2-methylfuran
10% 2-methylfuran in I	97.7	88.7	9.0	90% max iso-paraffin, 10% 2-methylfuran
20% 2-methylfuran in I	101.0	88.7	12.3	80% max iso-paraffin, 20% 2-methylfuran
30% 2-methylfuran in I	102.3	88.5	13.8	70% max iso-paraffin, 30% 2-methylfuran

10% isobutanol in O	94.6	86.0	8.6	90% max olefin, 10% isobutanol
20% isobutanol in O	97.0	86.8	10.2	80% max olefin, 20% isobutanol
30% isobutanol in O	99.1	87.3	11.8	70% max olefin, 30% isobutanol
10% isobutanol in N	93.1	85.7	7.4	90% max naphthene, 10% isobutanol
20% isobutanol in N	96.2	86.5	9.7	80% max naphthene, 20% isobutanol
30% isobutanol in N	98.5	87.1	11.4	70% max naphthene, 30% isobutanol
10% isobutanol in A	93.0	86.1	6.9	90% max aromatic, 10% isobutanol
20% isobutanol in A	96.2	87.2	9.0	80% max aromatic, 20% isobutanol
30% isobutanol in A	98.5	87.6	10.9	70% max aromatic, 30% isobutanol
10% isobutanol in P	94.3	86.3	8.0	90% max paraffin, 10% isobutanol
20% isobutanol in P	97.0	87.4	9.6	80% max paraffin, 20% isobutanol
30% isobutanol in P	99.3	88.1	11.2	70% max paraffin, 30% isobutanol
10% isobutanol in I	93.6	87.1	6.5	90% max iso-paraffin, 10% isobutanol
20% isobutanol in I	96.8	87.9	8.9	80% max iso-paraffin, 20% isobutanol
30% isobutanol in I	99.1	88.6	10.5	70% max iso-paraffin, 30% isobutanol
85 pump gas w/ethanol	90.4	82.2	8.2	85 AKA pump gasoline containing ethanol
87 pump gas w/ethanol	93.0	84.0	9.0	87 AKA pump gasoline containing ethanol
91 pump gas w/ethanol	96.8	85.3	11.5	91 AKA pump gasoline containing ethanol
91 pump gas no ethanol	92.6	86.3	6.3	91 AKA pump gasoline without ethanol
Pump racing fuel no ethanol	106.5	95.5	11.0	Pump racing fuel without ethanol
High-octane surrogate blend A	106.9	90.0	16.9	Surrogate blends comprising triptane, cyclopentane, diisobutylene, and ethylbenzene
High-octane surrogate blend B	107.7	91.4	16.3	
High-octane surrogate blend C	108.6	92.6	16.0	
High-octane surrogate blend D	105.0	88.0	17.0	
High-octane surrogate blend E	106.9	90.9	16.0	

475

476 **References**

[1] Edgar G. Measurement of knock characteristics of gasoline in terms of a standard fuel. Ind Eng Chem 1927;19:145–146. doi:10.1021/ie50205a049.

[2] ASTM International. ASTM D2700-19, Standard Test Method for Motor Octane Number of Spark-Ignition Engine Fuel. ASTM International: West Conshohocken, PA, 2019. http://www.astm.org/cgi-bin/resolver.cgi?D2700.

[3] ASTM International. ASTM D2699-19, Standard Test Method for Research Octane Number of Spark-Ignition Engine Fuel, ASTM International, West Conshohocken, PA, 2019, http://www.astm.org/cgi-bin/resolver.cgi?D2699.

[4] Splitter D, Pawlowski A, Wagner R. A Historical Analysis of the Co-evolution of Gasoline Octane Number and Spark-Ignition Engines. Front Mech Eng 2016;1:16. doi: 10.3389/fmech.2015.00016.

[5] Mittal V, Heywood J. The Shift in Relevance of Fuel RON and MON to Knock Onset in Modern SI Engines Over the Last 70 Years. SAE Int J Engines 2010;2(2):1–10. https://doi.org/10.4271/2009-01-2622.
[6] Kalghatgi G. Fuel Anti-Knock Quality - Part I. Engine Studies. SAE Technical Paper 2001-01-3584, 2001. https://doi.org/10.4271/2001-01-3584.
[7] Kalghatgi G. Fuel Anti-Knock Quality- Part II. Vehicle Studies - How Relevant is Motor Octane Number (MON) in Modern Engines? SAE Technical Paper 2001-01-3585, 2001. https://doi.org/10.4271/2001-01-3585.
[8] Szybist J, Busch S, McCormick R, Pihl J, Splitter D, Ratcliff M, Kolodziej C, Storey J, Moses-DeBusk M, Vuilleumier D, Sjöberg M, Sluder C, Rockstroh T, Miles P. What fuel properties enable higher thermal efficiency in spark-ignited engines?. Progress in Energy and Combustion Science 2021;82:100876. https://doi.org/10.1016/j.pecs.2020.100876.
[9] Leppard W. The chemical origin of fuel octane sensitivity. SAE Trans 1990;99:862–876. doi:10.4271/902137.
[10] Westbrook CK, Mehl M, Pitz WJ, Sjöberg M. Chemical kinetics of octane sensitivity in a spark-ignition engine. Combustion and Flame 2017;175:2–15. https://doi.org/10.1016/j.combustflame.2016.05.022.
[11] ASTM International. ASTM D613-18a, Standard Test Method for Cetane Number of Diesel Fuel Oil. ASTM International: West Conshohocken, PA, 2018.
[12] ASTM International. ASTM D6890-18, Standard Test Method for Determination of Ignition Delay and Derived Cetane Number (DCN) of Diesel Fuel Oils by Combustion in a Constant Volume Chamber. West Conshohocken, PA, 2018.
[13] ASTM International. ASTM D7668-17, Standard Test Method for Determination of Derived Cetane Number (DCN) of Diesel Fuel Oils—Ignition Delay and Combustion Delay Using a Constant Volume Combustion Chamber Method. West Conshohocken, PA, 2017.
[14] ASTM International. ASTM D8183-18, Standard Test Method for Determination of Indicated Cetane Number (ICN) of Diesel Fuel Oils using a Constant Volume Combustion Chamber—Reference Fuels Calibration Method. ASTM International: West Conshohocken, PA, 2018.
[15] Naser N, Yang SY, Kalghatgi G, Chung SH. Relating the octane numbers of fuels to ignition delay times measured in an ignition quality tester (IQT). Fuel 2017;187:117–127. https://doi.org/10.1016/j.fuel.2016.09.013.
[16] Naser N, Sarathy SM, Chung SH. Ignition delay time sensitivity in ignition quality tester (IQT) and its relation to octane sensitivity. Fuel 2018;233:412–419. https://doi.org/10.1016/j.fuel.2018.05.131.
[17] Luecke J, Rahimi M, Zigler B, Grout R. Experimental and numerical investigation of the Advanced Fuel Ignition Delay Analyzer (AFIDA) constant-volume combustion chamber as a research platform for fuel chemical kinetic mechanism validation. Fuel 2020;265:116929. https://doi.org/10.1016/j.fuel.2019.116929.
[18] Kolodziej C, Kodavasal J, Ciatti S, Som S, Shidore N, Delhom J. Achieving Stable Engine Operation of Gasoline Compression Ignition Using 87 AKI Gasoline Down to Idle. SAE Technical Paper 2015. https://doi.org/10.4271/2015-01-0832.
[19] Seidenspinner P, Härtl M, Wilharm T, Wachtmeister G. Cetane Number Determination by Advanced Fuel Ignition Delay Analysis in a New Constant Volume Combustion Chamber. SAE Technical Paper 2015-01-0798, 2015. https://doi.org/10.4271/2015-01-0798.
[20] McCormick RL, Fouts LA, Fioroni GM, Christensen ED, Ratcliff MA, Zigler BT, et al. Co-Optimization of Fuels & Engines: Properties of Co-Optima Core Research Gasolines. National Renewable Energy Laboratory: Golden, CO, 2018. doi:10.2172/1467176.
[21] Bogin GE, Luecke J, Ratcliff MA, Osecky E, Zigler BT. Effects of iso-octane/ethanol blend ratios on the observance of negative temperature coefficient behavior within the Ignition Quality Tester. Fuel 2016;186:82–90.
[22] Foong TM, Morganti KJ, Brear MJ, da Silva G, Yang Y, Dryer FL. The octane numbers of ethanol blended with gasoline and its surrogates. Fuel 2014;115:727–739. https://doi.org/10.1016/j.fuel.2013.07.105.